

# $m^6A$ transferase *METTL3* regulates endothelial-mesenchymal transition in diabetic retinopathy via *lncRNA SNHG7/KHSRP/MKL1* axis

Xin Cao<sup>\*</sup>, Yu Song, Li-Li Huang, Ya-Jing Tian, Xiao-Le Wang, Ling-Yan Hua

Department of Ophthalmology, Affiliated Hospital 2 of Nantong University, the first people's hospital of Nantong, Nantong 226000, Jiangsu Province, PR China

## ARTICLE INFO

### Keywords:

Diabetic retinopathy  
Endothelial-mesenchymal transition  
KHSRP  
SNHG7  
 $m^6A$   
METTL3  
MKL1

## ABSTRACT

Diabetic retinopathy is one of the microvascular complications in diabetic patients and the leading cause of blindness worldwide. The levels of METTL3, lncRNA SNHG7, KHSRP, MKL1, endothelial and mesenchymal markers were determined by RT-qPCR or western blot assays in vitro and in vivo. H&E staining was used to observe the retinal structure in a mouse model of DR. The expression levels of METTL3 and SNHG7 were significantly downregulated in DR patients, DR mice and high glucose-induced HRMECs cells. Notably, METTL3 installed the  $m^6A$  modification and enhanced the stability of SNHG7. Besides, METTL3 inhibited HRMECs EndoMT by promoting the expression of SNHG7. Additionally, SNHG7 was found to weaken MKL1 mRNA stability by binding to the RNA-binding protein KHSRP. Furthermore, we verified that METTL3 regulated EndoMT in DR through the SNHG7/MKL1 axis. We conclude that METTL3 regulates endothelial-mesenchymal transition in DR via the SNHG7/KHSRP/MKL1 axis, providing a new target for DR treatment.

## 1. Introduction

Diabetic retinopathy (DR) is one of the most serious microvascular complications of diabetes [1]. Despite advances in diagnosis and treatment, the prevalence of DR is increasing due to the high incidence of diabetes [2]. In severe cases, retinal hemorrhages, vitreous hemorrhage, and retinal detachment can occur, which can lead to permanent blindness in patients with DR [3]. Numerous studies have shown that hyperglycemia is the most common underlying factor leading to DR [4]. In addition, hyperglycemia impairs endothelial cell functions [5] and contributes to endothelial-mesenchymal transition (EndoMT) [6]. During the EndoMT process, injured endothelial cells lose the expression of cellular adhesion proteins (e.g., VE-Cadherin and CD31) and induce the expression of myofibroblast differentiation markers (e.g., SM-22 and FSP1) [7], as well as transcriptional factors (e.g., TWIST) [8]. Therefore, in-depth studies of the mechanism by which the EndoMT process is involved in DR are of great significance for the treatment of DR.

N6-methyladenosine ( $m^6A$ ) methylation is the most prevalent RNA modifications, and is associated with the development of multiple

diseases, including diabetes [9]. The  $m^6A$  RNA modification mediates its effect through its writer, reader, and eraser proteins, such as Methyltransferase-like 3 (METTL3), and is a possible candidate for controlling DR progression and pathogenesis [10]. METTL3 is an “writer” of  $m^6A$  modification and is essential for the regulation of  $m^6A$  methylation [11]. Recent data indicated that glucose regulated METTL3-mediated  $m^6A$  modifications in Type2 diabetes [12] and diabetic cataract [13]. Overexpression of METTL3 has been reported to alleviate the pyrolysis of retinal epithelial cells induced by high glucose [14]. Nevertheless, the function of METTL3 and its potential mechanism in EndoMT of DR remain unclear.

$m^6A$  can regulate the expression of long non-coding RNAs (lncRNAs) [15]. lncRNAs are composed of >200 nucleotides, acting as important genetic modulators [16]. Accumulating evidence indicates that numerous lncRNAs are involved in DR progression, such as lncRNA MEG3 and lncRNA H19 [17,18]. Small nucleolar RNA host gene 7 (SNHG7) is a crucial lncRNA that is located at chromosome 9q34.3 [19]. It has been shown that SNHG7 was downregulated in human retinal microvascular endothelial cells induced by high glucose, and its

**Abbreviations:** DR endothelial-mesenchymal transition EndoMT, diabetic retinopathy; FISH, fluorescence in situ hybridization; GCL, ganglion cell layer; H&E staining, hematoxylin and eosin staining; HRMECs, human retinal microvascular endothelial cells; KHSRP, KH-type splicing regulatory protein; lncRNAs, long non-coding RNAs; MKL1, megakaryocytic leukemia 1; METTL3, methyltransferase-like 3;  $m^6A$ , N6-Methyladenosine; RIP, RNA immunoprecipitation; SNHG7, small nucleolar RNA host gene 7; STZ, streptozotocin; VE-CAD, VE-Cadherin.

<sup>\*</sup> Corresponding author at: Department of Ophthalmology, Affiliated Hospital 2 of Nantong University, the first people's hospital of Nantong, No.6, Haierxiang North Road, Nantong 226000, Jiangsu Province, PR China.

E-mail address: [caoxin512@163.com](mailto:caoxin512@163.com) (X. Cao).

<https://doi.org/10.1016/j.ygeno.2022.110498>

Received 2 November 2021; Received in revised form 24 August 2022; Accepted 25 September 2022

Available online 26 September 2022

0888-7543/© 2022 The Authors. Published by Elsevier Inc. This is an open access article under the CC BY-NC-ND license (<http://creativecommons.org/licenses/by-nc-nd/4.0/>).

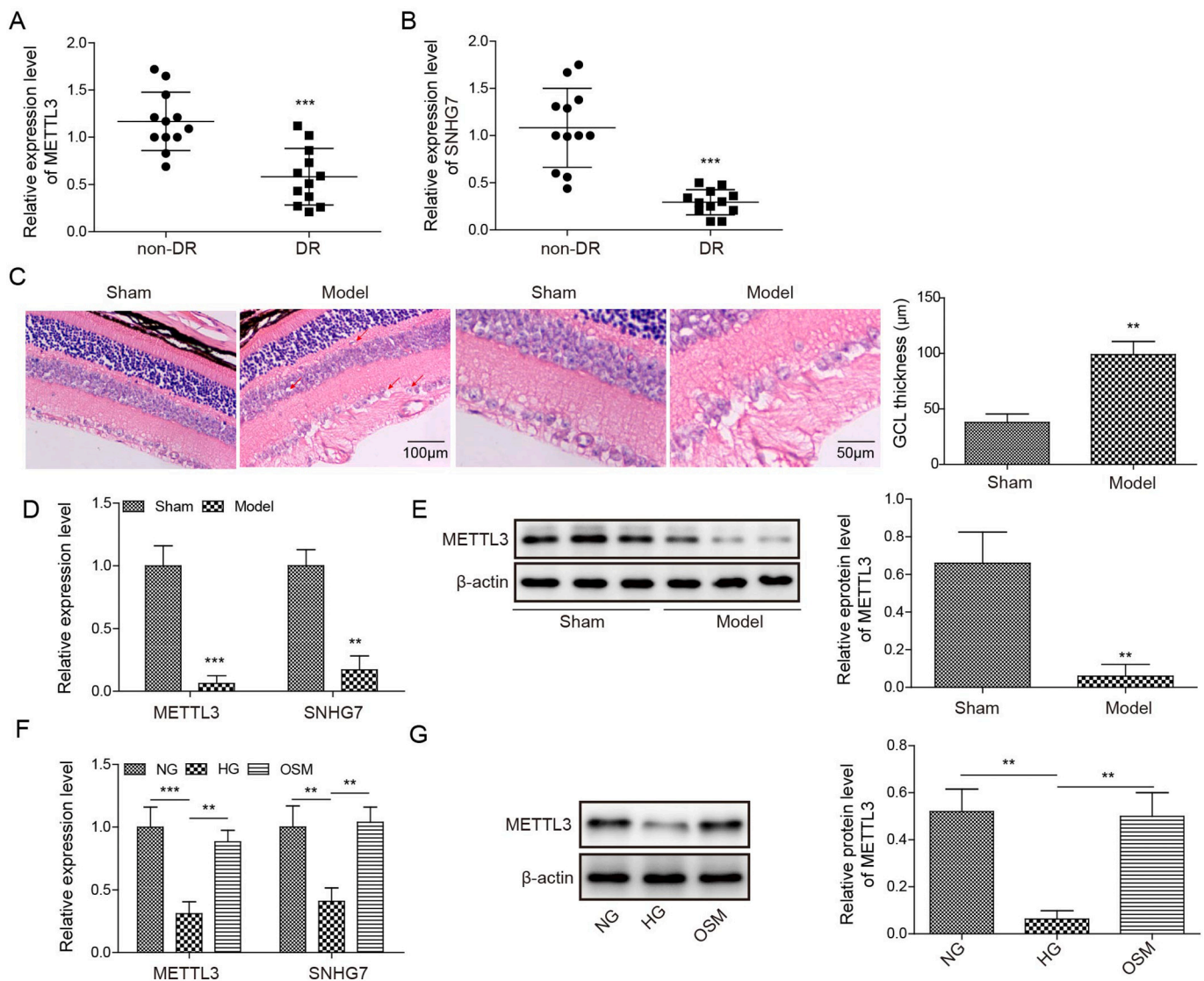


**Fig. 1.** Expression of METTL3 and SNHG7 in DR. (A, B) RT-qPCR was used to determine the expression of METTL3 and SNHG7 in vitreous humor samples from patients with DR or non-diabetic eye diseases (non-DR). (C) H&E staining was conducted to detect the retinal structures and thickness of ganglion cell layer (GCL) of DR mice and Sham mice. Scale bar, 100 μm, 50 μm. (D, E) The levels of METTL3 and SNHG7 in DR mice and Sham mice were analyzed by RT-qPCR or Western blot. (F, G) HRMECs were treated with normal glucose (NG, 5.5 mM), high glucose (HG, 25 mM) or hyperosmotic glucose (OSM, 35 mM). METTL3 and SNHG7 expression levels in cells were examined by RT-qPCR or Western blot. Data are the means  $\pm$  SD of triplicate experiments. \*\* $P$  < 0.01, \*\*\* $P$  < 0.001.

overexpression impaired the cell EndoMT [20]. In our preliminary study, we used the bioinformatics tool RMBase and found that SNHG7 has a potential m<sup>6</sup>A modification site, and the METTL3 motif is GGAC. However, whether METTL3 modifies SNHG7 expression in the process of DR needs further experimental verification.

Recent studies have shown that lncRNAs often regulate the stability of target mRNAs and participate in the disease process by interacting with RNA-binding proteins [21]. There is evidence that the expression of RNA-binding protein KH-type splicing regulatory protein (KHSRP) is downregulated in diabetes models [22]. Megakaryocytic leukemia 1 (MKL1) is a transcription modulator involved in the pathogenesis of human diseases [23]. Recently, it has been reported that MKL1 was highly expressed in retinal epithelial cells induced by high glucose, and MKL1 could promote EndoMT by activating TWIST1 [8,24]. In our study, bioinformatics tool StarBase predicted that SNHG7, MKL1 and KHSRP have potential binding relationships, suggesting that SNHG7 may affect the stability of MKL1 mRNA by interacting with KHSRP.

Therefore, this study aimed to explore the role of METTL3 in DR. We speculate that the m<sup>6</sup>A transferase METTL3 controls the EndoMT of DR

via the lncRNA SNHG7/KHSRP/MKL1 signaling axis. Our present study may imply a novel therapeutic target for the treatment of DR.

## 2. Results

### 2.1. METTL3 and SNHG7 were downregulated in DR

The present study first measured the expression of METTL3 and SNHG7 in vitreous humor samples from patients with DR or non-diabetic eye diseases by RT-qPCR. We found that the levels of METTL3 and SNHG7 were decreased obviously in DR patients compared to normal controls (Fig. 1A and B). Next, we constructed a mouse DR model. H&E staining showed that the retinal structure of mice in the sham group was clear and arranged in an orderly manner with normal morphology. In contrast, in DR mice, the retinal endothelium was markedly swollen, with disorganized cell distribution and localized dilation of blood vessels (Fig. 1C). We also discovered that METTL3 and SNHG7 were dramatically downregulated in the mouse model of DR compared with the control group (Fig. 1D and E). In addition, human

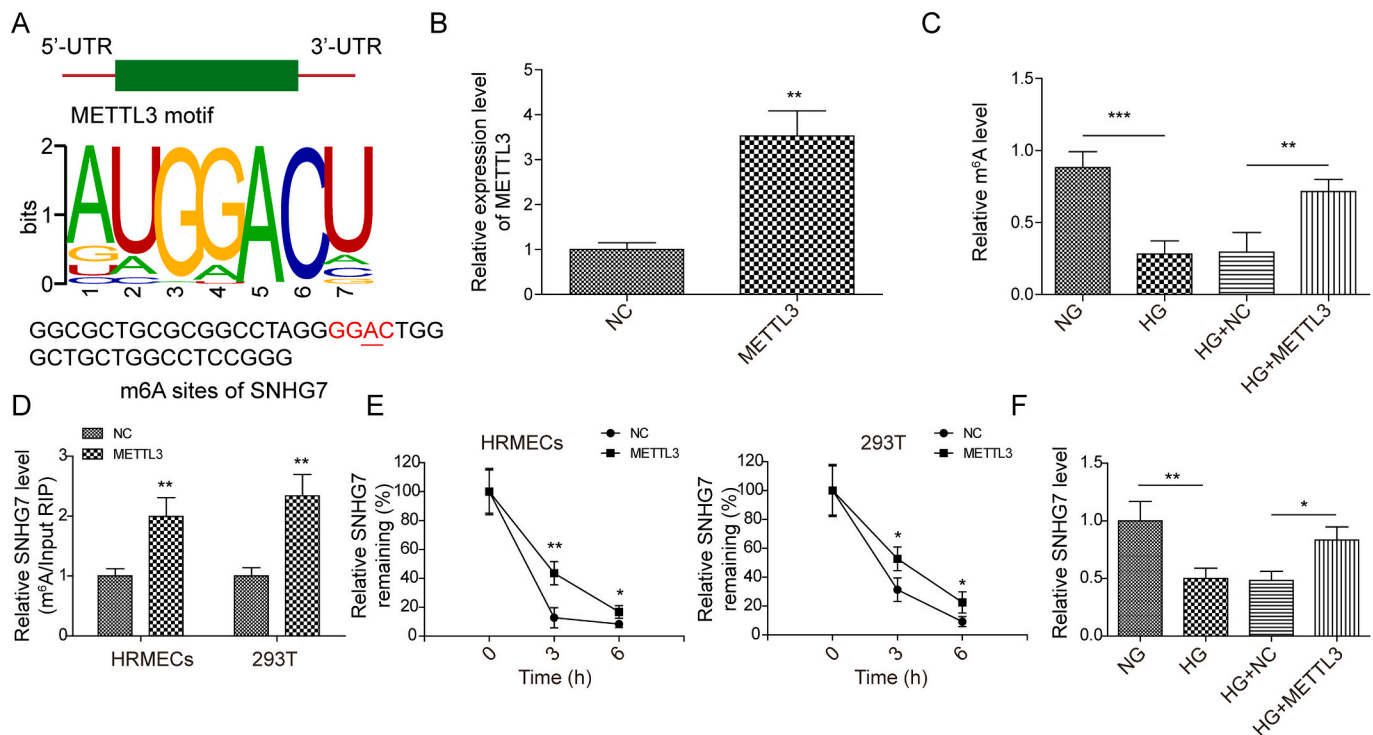


**Fig. 2.** METTL3 installed the m<sup>6</sup>A modification and increased the stability of SNHG7. (A) Prediction of the m<sup>6</sup>A modification site of SNHG7 by bioinformatics tool RMBase. (B) HRMECs were transfected with pcDNA3.1-METTL3 or negative control. The transfection level was detected by RT-qPCR. (C) The m<sup>6</sup>A levels were measured in different groups. (D) HRMECs or 293T cells were transfected with pcDNA3.1-METTL3 or negative control. RIP-qPCR demonstrated that SNHG7 had m<sup>6</sup>A modification in cells overexpressing METTL3. (E) Cells were treated with 5  $\mu$ g/mL actinomycin D for 0, 3, 6 h respectively. RT-qPCR was conducted to analyze the stability of SNHG7. (F) The expression of SNHG7 was determined by RT-qPCR. Data are the means  $\pm$  SD of triplicate experiments. \* $P$  < 0.05, \*\* $P$  < 0.01, \*\*\* $P$  < 0.001.

retinal microvascular endothelial cells (HRMECs) were treated with normal glucose (NG), high glucose (HG) or hyperosmotic glucose (OSM). The results of RT-qPCR and Western blot revealed that METTL3 and SNHG7 were extremely low in high glucose-induced HRMECs compared with the NG and OSM groups (Fig. 1F and G). Collectively, these data suggest that METTL3 and SNHG7 are lowly expressed in DR, and there may be a regulatory relationship between METTL3 and SNHG7.

## 2.2. METTL3 installed the m<sup>6</sup>A modification and increased the stability of SNHG7

To further evaluate the relationship between METTL3 and SNHG7, we used RMBase (<http://rna.sysu.edu.cn/rmbase/m6Amod.php>) for bioinformatic analysis. As illustrated in Fig. 2A, SNHG7 has a potential m<sup>6</sup>A modification site, and the METTL3 motif is GGAC. Furthermore, we determined METTL3 expression in HRMECs with pcDNA3.1-METTL3 and found that METTL3 overexpression had a dramatic effect on METTL3 level (Fig. 2B). Besides, overexpression of METTL3 greatly increased m<sup>6</sup>A level in HG-induced HRMECs (Fig. 2C). Importantly, METTL3 upregulation obviously promoted SNHG7 m<sup>6</sup>A modification and enhanced the stability of SNHG7 RNA in both HRMECs and 293T cells (Fig. 2D and E). Meanwhile, overexpression of METTL3 significantly induced the expression of SNHG7 in cells stimulated by HG (Fig. 2F). Thus, the above results reveal that METTL3 installs the m<sup>6</sup>A modification and induces the stability of SNHG7.

## 2.3. METTL3 inhibited HRMECs EndoMT by upregulating SNHG7 expression

To study the biological functions of METTL3 in DR development, we transfected pcDNA3.1-METTL3 and sh-SNHG7 into HRMECs, and

stimulated cells with HG. With SNHG7 silencing, the SNHG7 level was obviously decreased compared to the control (Fig. 3A). Meanwhile, HG resulted in a significant decrease of SNHG7, VE-Cadherin (VE-CAD) and CD31, as well as a significant increase of FSP1, SM22 and TWIST1, which were all reversed by the overexpression of METTL3. However, suppression of SNHG7 could partially overturn the effects of METTL3 (Fig. 3B-D). Moreover, immunofluorescence for VE-CAD and SM22 showed the same trend as the above results (Fig. 3E). Taken together, these findings indicate that METTL3 represses EndoMT in HRMECs by upregulating SNHG7 expression.

## 2.4. SNHG7 interacted with RNA-binding protein KHSRP and increased its expression

We further explored the molecular mechanism by which SNHG7 regulates DR and identified that SNHG7 was distributed in both the nucleus and cytoplasm of HRMECs, mainly in the nucleus (Fig. 4A and B). Meanwhile, RNA-binding protein KHSRP was predicted to be a downstream target of SNHG7 by the bioinformatics tool StarBase (<https://starbase.sysu.edu.cn/>). RNA pull-down and RIP assays further verified the binding of SNHG7 to KHSRP in both HRMECs and 293T cells (Fig. 4C and D). Moreover, the level of SNHG7 was greatly elevated in HRMECs with pcDNA3.1-SNHG7 (Fig. 4E). Additionally, KHSRP expression was obviously increased in HRMECs with SNHG7 overexpression, compared to the control group. When SNHG7 was inhibited, the expression of KHSRP was suppressed (Fig. 4F and G). Collectively, the above findings demonstrate that SNHG7 increases KHSRP expression by directly targeting it.



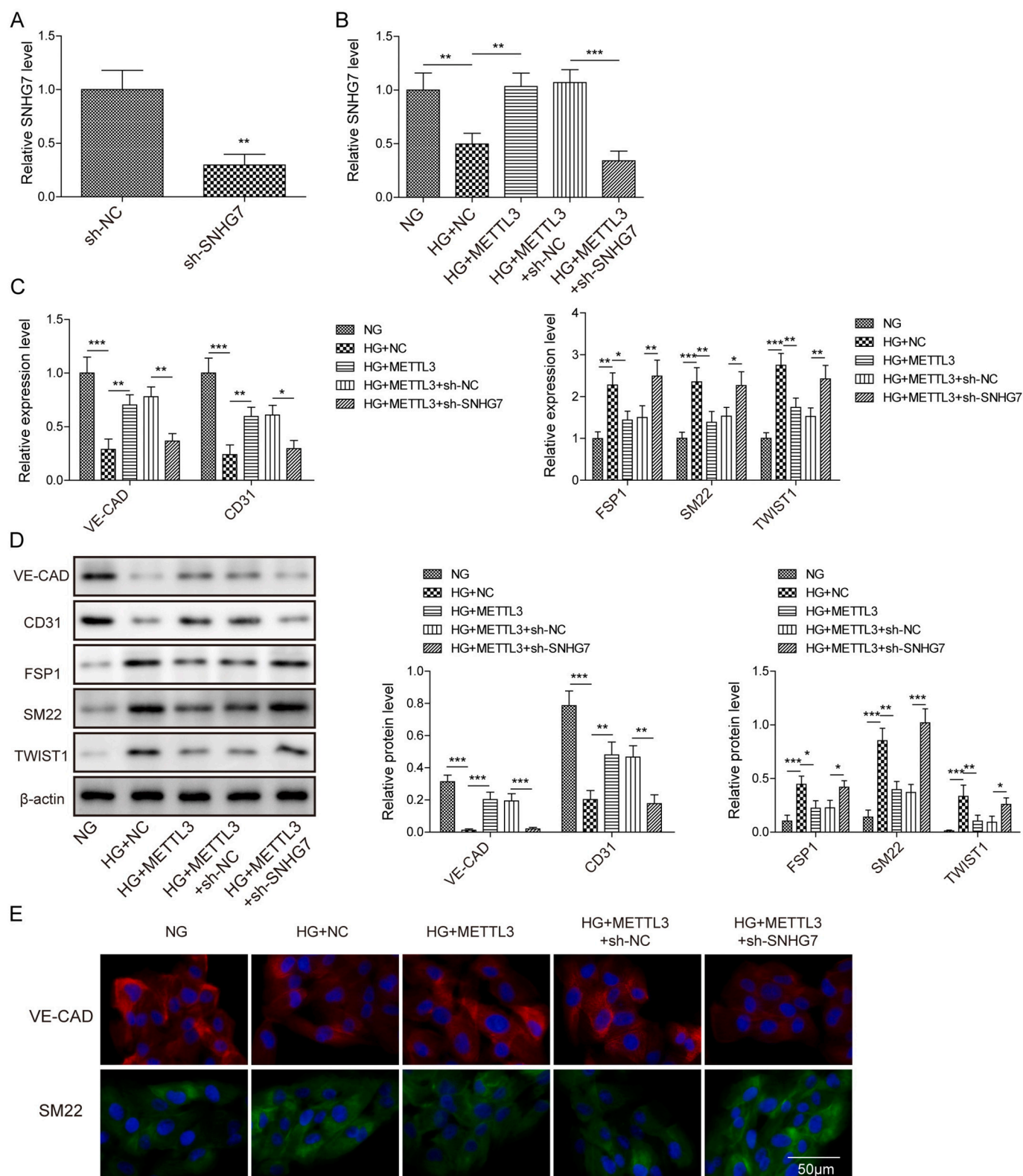


**Fig. 3.** METTL3 inhibited HRMECs EndoMT by upregulating SNHG7 expression. HRMECs were transfected with pcDNA3.1-METTL3 and sh-SNHG7, and stimulated with HG. (A, B) The expression of SNHG7 was tested by RT-qPCR. (C, D) The levels of EndoMT markers (VE-CAD, CD31, FSP1, SM22, TWIST1) were measured by RT-qPCR and Western blot. (E) Immunofluorescence analysis of VE-CAD and SM22 expression in HRMECs. Scale bar: 50  $\mu$ m. Data are the means  $\pm$  SD of triplicate experiments. \* $P$  < 0.05, \*\* $P$  < 0.01, \*\*\* $P$  < 0.001.



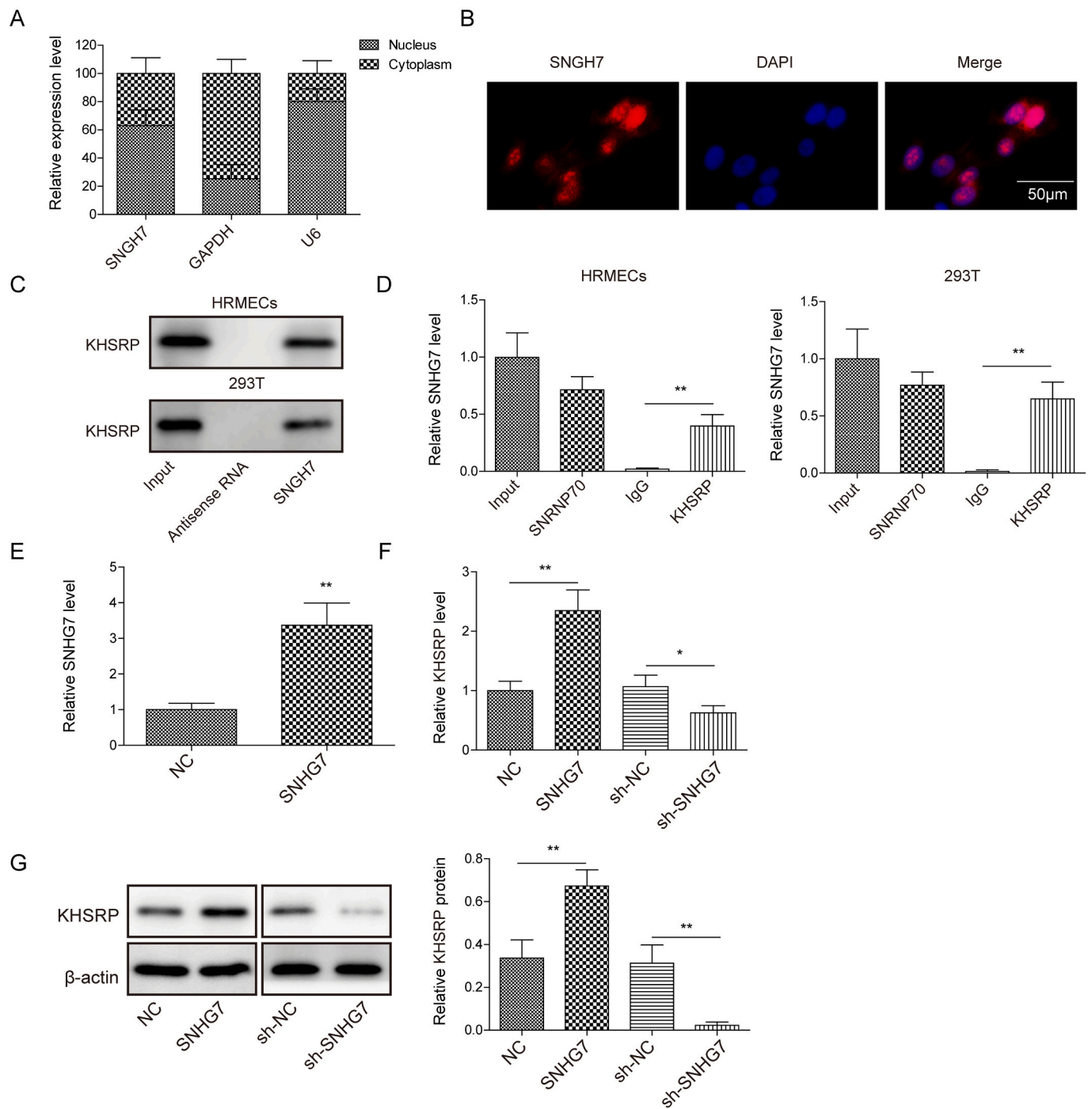


**Fig. 4.** SNHG7 increased KHSRP expression by directly targeting it. (A, B) Subcellular fractionation assay and RNA FISH assay was performed to detect the expression and location of SNHG7 in HRMECs. (C) RNA pull down assay was utilized to verify the binding of SNHG7 to KHSRP. (D) RIP assay revealed the relationship between SNHG7 and KHSRP. (E) RT-qPCR analysis of SNHG7 level. (F, G) The expression of KHSRP was determined by RT-qPCR and Western blot. Data are the means  $\pm$  SD of triplicate experiments. \* $P < 0.05$ , \*\* $P < 0.01$ .

## 2.5. SNHG7 attenuated the stability of MKL1 mRNA by binding to KHSRP

The bioinformatics tool StarBase also predicted that KHSRP has a binding site to MKL1. RT-qPCR analysis demonstrated that KHSRP was decreased, while MKL1 expression was increased in vitreous humor samples from DR patients compared with that in normal subjects (Fig. 5A). Moreover, RNA pull-down and RIP assays revealed that KHSRP and MKL1 have a binding relationship (Fig. 5B and C). When we transfected HRMECs with pcDNA3.1-KHSRP or sh-KHSRP, the effects of

KHSRP overexpression and knockdown were significant (Fig. 5D). Additionally, SNHG7 and KHSRP negatively regulated the expression of MKL1 (Fig. 5E and F). Besides, the stability of MKL1 RNA was obviously impaired by overexpression of SNHG7 and KHSRP in both HRMECs and 293T cells (Fig. 5G). Hence, these results indicate that SNHG7 attenuates the stability of MKL1 mRNA through KHSRP.

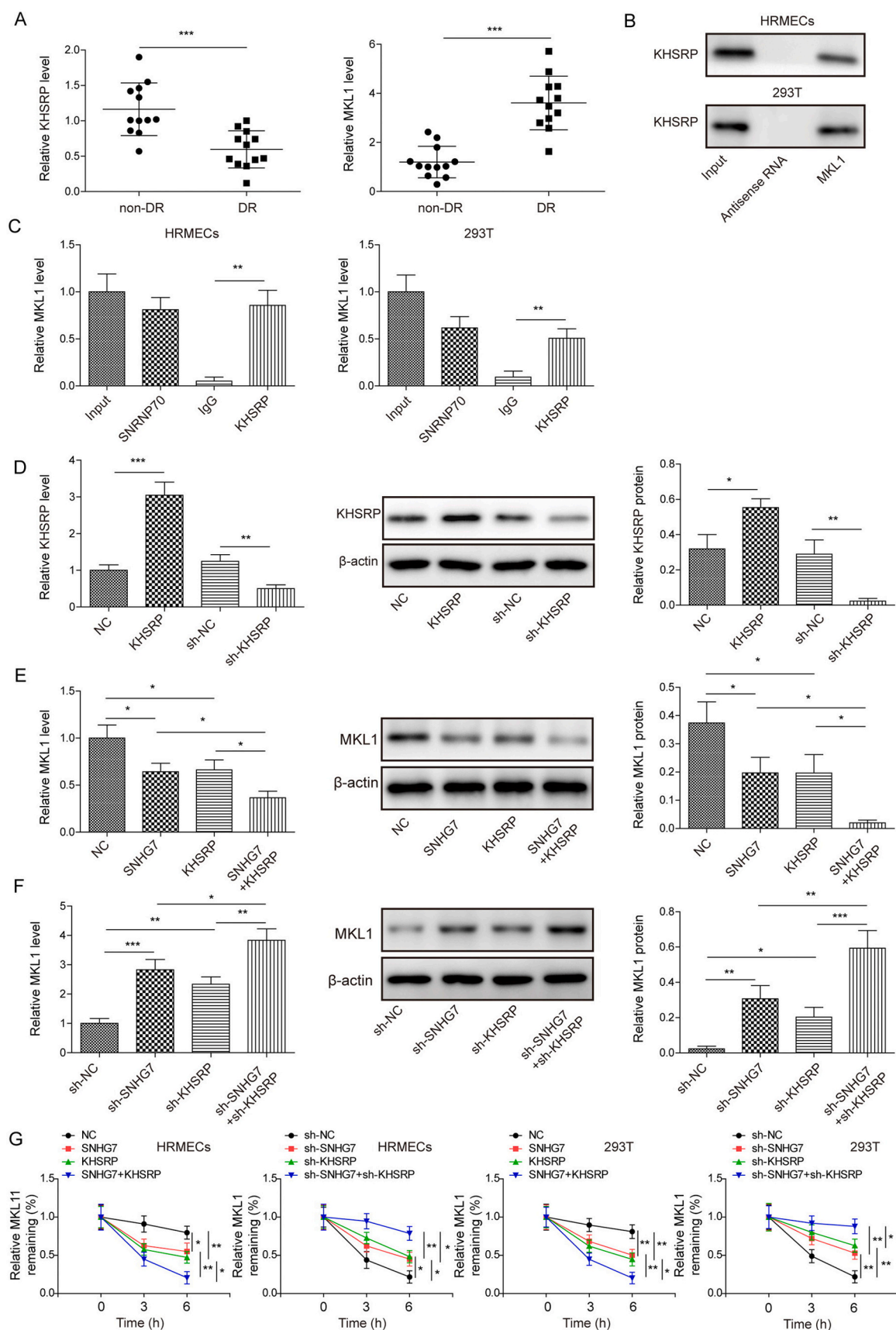


**Fig. 5.** SNHG7 attenuated the stability of MKL1 mRNA by binding to KHSRP. (A) RT-qPCR analysis of KHSRP and MKL1 in vitreous humor samples of DR patients. (B) RNA pull down assay identified the binding of MKL1 to KHSRP. (C) RIP assay verified the relationship between KHSRP and MKL1. (D–F) The expression of KHSRP or MKL1 was tested by RT-qPCR and Western blot in each group. (G) Cells were treated with 5  $\mu$ g/mL actinomycin D for 0, 3, 6 h respectively. RT-qPCR was used to detect the stability of MKL1. Data are the means  $\pm$  SD of triplicate experiments. \* $P < 0.05$ , \*\* $P < 0.01$ , \*\*\* $P < 0.001$ .

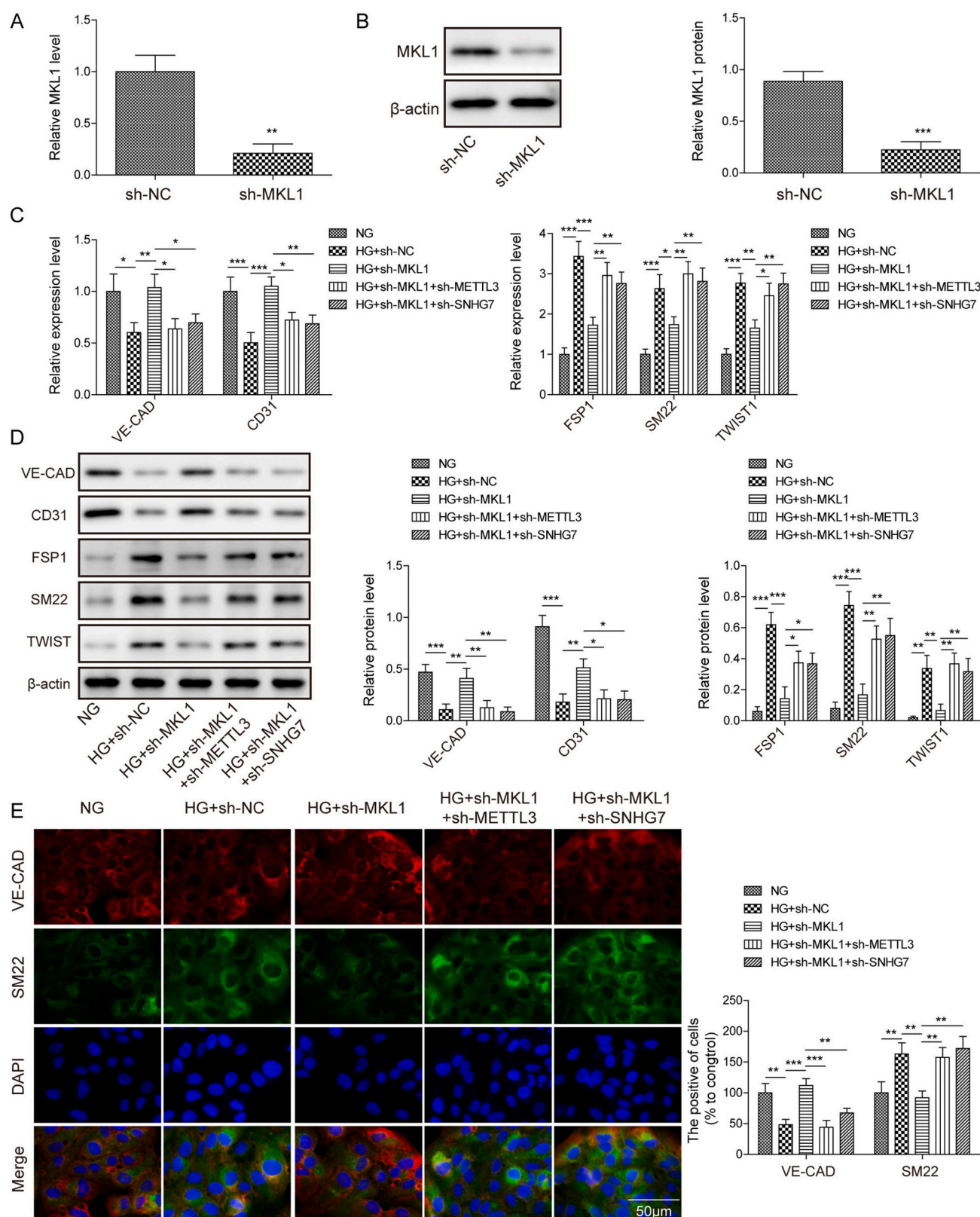


**Fig. 6.** Knockdown of METTL3 or SNHG7 reversed the effect of MKL1 silencing on EndoMT of HRMECs. (A, B) HRMECs were transfected with sh-MKL1 or negative control. MKL1 level was measured by RT-qPCR or Western blot. (C, D) HRMECs were transfected with sh-MKL1, sh-METTL3, sh-SNHG7 or negative control, and treated with HG. The levels of EndoMT markers (VE-CAD, CD31, FSP1, SM22, TWIST1) were assessed by RT-qPCR and Western blot. (E) Double immunofluorescence staining of HRMECs using antibodies against VE-CAD (red) and SM22 (green). Scale bar: 50 μm. Data are the means ± SD of triplicate experiments. \**P* < 0.05. (For interpretation of the references to colour in this figure legend, the reader is referred to the web version of this article.)



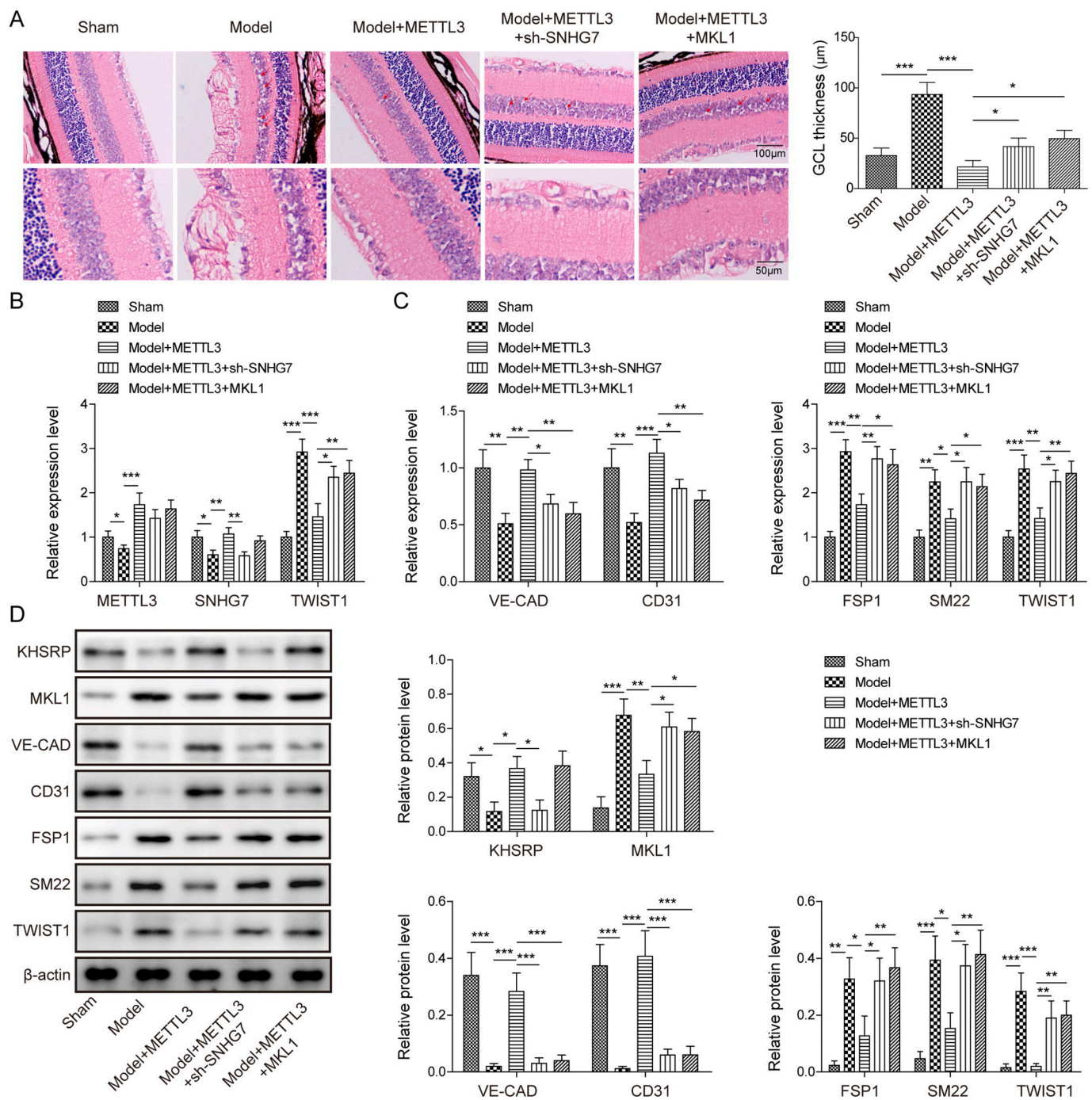


**Fig. 7.** METTL3 regulated EndoMT in DR mice through the SNHG7/MKL1 axis. DR mice were treated with pcDNA3.1-METTL3, sh-SNHG7 and pcDNA3.1-MKL1. (A) The retinal structures and thickness of ganglion cell layer (GCL) of DR mice and Sham mice were detected by H&E staining. Scale bar: 100 μm, 50 μm. (B) RT-qPCR analysis of METTL3, SNHG7 and MKL1 expression in DR mice and Sham mice. (C, D) The levels of EndoMT markers (VE-CAD, CD31, FSP1, SM22, TWIST1) were measured by RT-qPCR and Western blot. Data are the means ± SD of triplicate experiments. \**P* < 0.05.

## 2.6. Knockdown of METTL3 or SNHG7 reversed the effect of MKL1 silencing on EndoMT of HRMECs

We further investigated the effects of MKL1 on EndoMT in HRMECs. There was a decrease of MKL1 expression in cells with MKL1 silencing, compared to the control cells (Fig. 6A and B). It was found that HG remarkably reduced the expression of VE-CAD and CD31, and induced the level of FSP1, SM22 and TWIST1, whereas knockdown of MKL1 greatly suppressed the effects of HG on the expression of these EndoMT markers. Nevertheless, METTL3 or SNHG7 silencing could partially

reverse these effects of sh-MKL1 (Fig. 6C and D). Meanwhile, the results of double immunofluorescence staining showed low expression of VE-CAD (red) and high expression of SM22 (green) in HG-treated cells, whereas such effects were lost by transfection of sh-MKL1 in HG-treated cells. However, these effects were restored by co-transfection of sh-MKL1 with sh-METTL3 or sh-SNHG7 in HG-treated cells (Fig. 6E). Altogether, these findings demonstrate that knockdown of METTL3 or SNHG7 reverses the effect of MKL1 silencing on EndoMT of HRMECs.

## 2.7. METTL3 regulated EndoMT in DR mice through the SNHG7/MKL1 axis

To illustrate whether METTL3 could alleviate DR progression in vivo, we treated DR mice by injecting lentivirus expressing pcDNA3.1-METTL3, sh-SNHG7, pcDNA3.1-MKL1 or control vectors through vitreous chamber of mice. The retinal morphological changes were detected by H&E staining. As shown in Fig. 7A, the retinal structure was disrupted in DR mice and was remarkably improved by METTL3 overexpression, whereas SNHG7 silencing or MKL1 overexpression partially abolished the effect of METTL3 upregulation on retinal structure. As expected, in DR mice, METTL3 and SNHG7 was downregulated, while MKL1 was upregulated compared with the Sham mice. Knockdown of SNHG7 or overexpression of MKL1 could partially reverse the regulation of MKL1 expression by METTL3 overexpression (Fig. 7B). In addition, compared to the Sham mice, VE-CAD and CD31 levels were reduced, whereas FSP1, SM22 and TWIST1 levels were elevated in DR mice, and this change was repressed by overexpressed METTL3. Conversely, SNHG7 silencing or MKL1 overexpression could partially overturn the expression of EndoMT-related molecules regulated by METTL3 (Fig. 7C and D). Taken together, these results indicate that METTL3 controls EndoMT in DR mice via the SNHG7/MKL1 signaling pathway.

## 3. Discussion

Diabetic retinopathy (DR) is one of the more serious complications of diabetes and a common blinding eye disease [25]. In recent years, with the increase of diabetic patients and the extension of human lifespan, the visual impairment caused by DR has gradually increased [26]. Endothelial cells undergoing EndoMT contribute to the loss of vision in DR patients [20,27]. Therefore, identifying the molecular mechanisms underlying EndoMT in DR is very important for its earlier detection and treatment. In this study, we demonstrated that m<sup>6</sup>A transferase METTL3 could regulate EndoMT in DR via the lncRNA SNHG7/KHSRP/MKL1 axis.

Methylation of m<sup>6</sup>A, the most common RNA methylation, is thought to be critical in a range of biological processes [28]. Accumulated evidence indicates that m<sup>6</sup>A RNA modification plays an important regulatory role in DR [10]. As a major writer of m<sup>6</sup>A methylation, METTL3 can affect tumor formation by regulating m<sup>6</sup>A modification [29]. Xu et al. reported that METTL3 attenuated high glucose-induced pyroptosis in RPE cells via the miR-25-3p/Pten/Akt axis [14]. Furthermore, METTL3 mediated-m<sup>6</sup>A modification is closely associated with the development of type 2 diabetes [12]. Besides, METTL3 can modulate various biological processes via interacting with lncRNAs [30,31]. In accordance with these previous researches, our study revealed that METTL3 and lncRNA SNHG7 were low expressed in the vitreous humor samples of DR patients and DR mice, as well as high glucose-induced HRMECs. In addition, overexpression of METTL3 repressed EndoMT in HG induced-HRMECs through inducing the stability and expression of SNHG7. Similarly, Cao et al. demonstrated that SNHG7 suppressed EndMT and tube formation in HRMECs via the miR-34a-5p/XBP1 axis [20]. Thus, our results indicated that METTL3 might participate in the regulation of DR development. Recently, METTL3 has been demonstrated to be an angiogenic regulator. For example, Yao et al. reported that METTL3 promoted endothelial cell viability, proliferation, migration by regulating Wnt signaling through the m<sup>6</sup>A modification of target genes [32]. Jiang et al. found that METTL3 accelerated bone regeneration by enhancing endothelial progenitor cell angiogenesis via the PI3K/AKT pathway [33]. Therefore, further study is needed to determine whether METTL3 can induce angiogenesis during DR.

The literature suggests that lncRNA and RNA-binding proteins can form complexes to regulate downstream gene expression [34]. KHSRP is a novel RNA-binding protein implicated in cell differentiation and disease [35]. Gou et al. showed that lncRNA AB074169 impaired cell proliferation through KHSRP in papillary thyroid carcinoma [36].

Similar to previous studies, we found that SNHG7 was associated with KHSRP and promoted its expression. Further bioinformatics revealed that MKL1 could also be a target of KHSRP. MKL1 is aberrantly expressed in various diseases, including diabetes [37]. Deletion of MKL1 in mice could alleviate diabetic nephropathy [38]. Our study illustrated that KHSRP was downregulated, while MKL1 expression was upregulated in vitreous humor samples from DR patients. We further confirmed that KHSRP and MKL1 had a binding relationship by RNA pull-down and RIP assays. Subsequently, we identified that SNHG7 and KHSRP overexpression obviously reduced the stability of MKL1 mRNA in both HRMECs and 293T cells. Taken together, the above results revealed that SNHG7 attenuated the stability of MKL1 mRNA by binding to KHSRP.

Functional assays further demonstrated that MKL1 downregulation greatly suppressed EndoMT in HG-induced HRMECs. On the other hand, knockdown of METTL3 or SNHG7 reversed the effect of MKL1 silencing on EndoMT of HRMECs. Similarly, in vivo experiments revealed that METTL3 controlled EndoMT through the SNHG7/MKL1 axis in DR mice. These data confirmed the previous reports that MKL1 served a key role in EndoMT by activating TWIST1 [8] and SNHG7 inhibited EndoMT in DR [20]. More importantly, our results suggested that METTL3 modulated the progression of DR via the SNHG7/MKL1 signaling pathway.

## 4. Materials and methods

### 4.1. Clinical specimens

Human vitreous humor samples from patients with DR ( $n = 12$ ) or non-diabetic eye diseases (non-DR,  $n = 12$ ) were obtained from individuals who underwent plana vitrectomy at Affiliated Hospital 2 of Nantong University, the first people's hospital of Nantong from September 2017 to October 2019. All experiments were conducted with the approval of the Clinical Research Ethics Committee of Affiliated Hospital 2 of Nantong University, the first people's hospital of Nantong. Written informed consent was provided by the patients.

### 4.2. Animal models establishment

Male C57/BL6J mice (8–10 weeks old, 200–220 g weight) were purchased from Shanghai Laboratory Animal Center (Shanghai, China). Mice were maintained in a Specific-pathogen-free lab with temperature (22–23 °C), humidity (55–60%) and a 12 h light (7:00)/dark (19:00) cycle. Streptozotocin (STZ) was dissolved in 0.1 M citrate acid buffer (pH 4.0, Sigma, St. Louis, MO, USA). Diabetes was induced by intraperitoneal injection of 50 mg/kg STZ for 5 consecutive days. Normal control mice were administered sodium citrate buffer. Seven days later, the blood from the tail vein was used for the measurement of glucose level. Mice diabetes model was considered to be successful when the blood glucose was  $>16$  mmol/L and maintained for over one week. Lentivirus expressing pcDNA3.1-METTL3, sh-SNHG7, pcDNA3.1-MKL1 and negative control oligonucleotides were obtained from GenePharma (Shanghai, China). At one week following the induction of diabetes, mice were randomly grouped. The corresponding lentivirus were injected into the vitreous cavity of each group of mice [39]. After 4 weeks, the mice were euthanized by isoflurane and retinal tissues were stored in liquid nitrogen. All protocols of animal experiments were carried out according to the Guide for the Care and Use of Laboratory Animals of the Chinese National Institutes of Health. The current study was approved by the Animal Ethics Committee of Affiliated Hospital 2 of Nantong University, the first people's hospital of Nantong.

### 4.3. Cell culture and treatment

Human retinal microvascular endothelial cells (HRMECs) were provided by the PriCells Biotechnological Co., Ltd. (Wuhan, China) and 293T cells were obtained from the American Type Culture Collection (ATCC, Manassas, VA, USA). Cells were cultured in Dulbecco's modified

Eagle's medium (DMEM, Invitrogen, Carlsbad, CA, USA) with 10% fetal bovine serum (Invitrogen), penicillin (100 U/mL) and streptomycin (100 U/mL) at 37 °C under 5% CO<sub>2</sub>.

#### 4.4. Cell transfection

After 24 h of incubation with serum-free DMEM, HRMECs were treated with normal glucose (NG, 5.5 mM), high glucose (HG, 25 mM) or hyperosmotic glucose (OSM, 35 mM). The short hairpin RNA for METTL3, SNHG7, KHSRP, MKL1 and the scrambled controls were designed and synthesized by GenePharma (Shanghai, China). The cDNA fragments for METTL3, KHSRP and MKL1, and the sequence of SNHG7 were amplified and cloned into pcDNA3.1 vectors, which were constructed by GenePharma (Shanghai, China). Transfection was performed using Lipofectamine 2000 reagent (Invitrogen) in HRMECs as described previously [40]. Briefly, cells were seeded at  $7.5 \times 10^5$  cells/mL to achieve 90% confluence. 100 µM of each construct was used to transfect the cells for 4 h and subsequently recovered in full medium overnight. The following morning, cells were serum starved for 24 h and were then treated with glucose as above for 48 h. The transfection efficiency of knockdown constructs was confirmed using RT-qPCR. All knockdown constructs demonstrated similar knockdown activity (65–75%) when compared to scrambled controls. Each experiment was performed with three or more replicates.

#### 4.5. m<sup>6</sup>A quantification

The extracted RNA was purified and quantified. Total RNA was then subjected to a Dynabeads mRNA Purification Kit (Thermo Fisher Scientific, Waltham, MA, USA) for mRNA purification. Later, the mRNA (200 ng/sample) was used for m<sup>6</sup>A quantification using a EpiQuik m<sup>6</sup>A Methylation Quantification kit (Colorimetric, ab185912, Epigentek, Farmingdale, NY, USA) according to the manufacturer's protocol. The m<sup>6</sup>A level was detected by reading the absorbance at 450 nm.

#### 4.6. Total RNA extraction, reverse transcription and real-time quantitative PCR

Trizol reagent (Invitrogen) was applied for isolating total RNA. RNA was reversely transcribed into cDNA using a PrimeScript™ RT Reagent Kit (Takara, Kyoto, Japan). The relative gene expression levels were determined using the SYBR Green PCR Kit (Takara) on an Applied Biosystems 7500 Real-Time PCR System (Applied Biosystems, Foster City, CA, USA). The primer sequences are listed as follows: METTL3 F: 5'-AGATGGGGTAGAAAGCCTCCT-3', R: 5'-TGGTCAGCATAGGTTACAA-GAGT-3'; SNHG7 F: 5'-AGGCTGGCTGGAATAAAGGT-3', R: 5'-TAT-GAAAAGGGAGGCGTGGT-3'; KHSRP F: 5'-GCAGCAGGCTCAATGAATCG-3', R: 5'-GTGAGACACAGAACAGGCGA-3'; MKL1 F: 5'-CCCAAAGGTAGCAGACAGTTC-3', R: 5'-GAGTGGGTGATATGGAGGTGG-3'; VE-Cadherin F: 5'-ATCGGTTGTTCAATGCGTCC-3', R: 5'-CCTTCAGGATTTGGTACATGACA-3'; CD31 F: 5'-ATTGCTCTGGTCACTTCTCC-3', R: 5'-CAGGCCCATTTGTTCC-3'; TWIST1 F: 5'-TCGGA-CAAGCTGAGCAAGAT-3', R: 5'-CCAGACGGAGAAGGCGTAG-3'. GAPDH was utilized as an internal control. We used the standard 2<sup>-ΔΔC<sub>t</sub></sup> method to determine the relative gene expression.

#### 4.7. RNA stability

Cells ( $2 \times 10^4$ /well) were plated in 12-well plates. After overnight incubation, cells were treated with 5 µg/mL actinomycin D (A9415, Sigma) for 0, 3, 6 h respectively. Cells were then collected and total RNA was isolated. RT-qPCR was used to determine the expression of SNHG7 and MKL1.

#### 4.8. Western blot

Prepared cells or tissues were added with RIPA lysis buffer to extract total protein. A total of 20 µg protein lysates were separated by 10% SDS-PAGE gels, transferred to PVDF membranes (Millipore, Boston, MA, USA), and blocked with 5% non-fat milk in TBST for 1 h. The membranes were then incubated with following primary antibodies at 4 °C overnight: METTL3 (1:1000, Abcam, Cambridge, MA, USA), KHSRP (1:500, Abcam), MKL1 (1:1000, Santa Cruz), VE-Cadherin (1:1000, Abcam), CD31 (1:200, Abcam), FSP1 (1:1000, Sigma), SM22 (1:1000, Thermo Fisher Scientific), TWIST1 (1:1000, Cell Signaling Technology, Danvers, MA, USA). Subsequently, the membranes were rinsed by TBST and incubated with horseradish peroxidase-conjugated secondary antibody (1:1000, Cell Signaling Technology) for 1 h at room temperature and developed using ECL system (GE Healthcare, UK). β-actin was utilized as an internal loading control. The density of the bands was quantified using the ImageJ software (National Institutes of Health, USA).

#### 4.9. Immunofluorescence

The transfected cells were fixed with 4% paraformaldehyde (Sigma) for 20 min. Next, cells were permeabilized with 0.2% Triton X-100 in PBS (Sigma) for 5 min. After blocking with blocking buffer containing 10% normal goat serum for 30 min, cells were probed by anti-VE-Cadherin antibody (1:50, Abcam, Cambridge, MA, USA) or anti-SM22 antibody (1:50, Abcam, Cambridge, MA, USA) at 4 °C overnight, following by incubation with FITC labeled IgG secondary antibody for 1 h at room temperature. Cells were then incubated with DAPI for 5 min and washed with PBS. Images were visualized with a fluorescence microscope (Olympus).

#### 4.10. Subcellular fractionation assay

The PARIS Kit (Thermo Fisher Scientific, USA) was used to detect the cellular localization of SNHG7 in nucleus and cytoplasm according to the manufacturer's protocol. Briefly, HRMECs were resuspended using cell fractionation buffer and then centrifuged. The cell disruption buffer was used to preserve nuclear precipitation and supernatant for RNA extraction. The expression of SNHG7 was measured by real-time PCR. GAPDH and U6 transcripts were utilized as internal markers.

#### 4.11. Fluorescence in situ hybridization (FISH)

In order to test the expression and localization of SNHG7, HRMECs were fixed with 4% paraformaldehyde for 20 min at room temperature and permeabilized using 0.5% Triton X-100 for 5 min. Cells were then blocked with pre-hybridization solution for 30 min at 37 °C. FISH analysis was performed using fluorescence labeled SNHG7 probe (Ribobio, Guangzhou, China) overnight at 37 °C. After washing, nuclei were stained with DAPI. Subsequently, images were visualized with a fluorescence microscope (Leica).

#### 4.12. RNA pull-down assay

RNA pull-down analysis was performed using the Pierce™ Magnetic RNA-Protein Pull-Down Kit (Thermo Fisher Scientific, USA). In brief, biotinylated SNHG7 or MKL1 was transfected into HRMECs and 293T cells. The cells were then incubated with streptavidin agarose beads (Invitrogen) for 2 h, followed by eluted with biotin elution buffer. The pulled down KHSRP RNA was detected by RT-qPCR.

#### 4.13. RNA immunoprecipitation assay

RNA immunoprecipitation (RIP) assay was conducted with the Magna RIP™ RNA-Binding Protein Immunoprecipitation Kit (Millipore). In brief, HRMECs or 293T cells were collected and lysed in RNA lysis



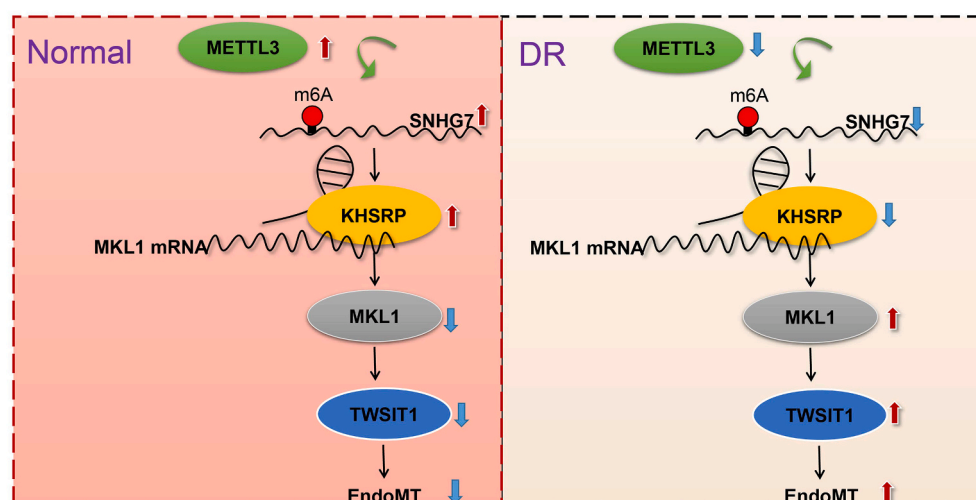


**Fig. 8.** The molecular mechanism by which METTL3 regulates EndoMT of DR. METTL3 and SNHG7 are downregulated in DR. METTL3 installs the m<sup>6</sup>A modification and upregulates the stability of SNHG7. SNHG7 weakens the stability of MKL1 mRNA by binding to KHSRP. In turn, METTL3 overexpression leads to an increase in endothelial markers and a reduction in mesenchymal markers, leading to the prevention of EndoMT in DR via the SNHG7/MKL1 axis.

buffer containing protease and RNase inhibitors. A portion of the cell lysis was isolated as the input. The other portion was incubated with magnetic beads conjugated with anti-KHSRP antibody (Cell Signaling Technology) at 4 °C overnight. Anti-IgG (Cell Signaling Technology) was utilized as a normal control and anti-SNRNP70 (Cell Signaling Technology) was used as a positive control. The samples were then digested with proteinase K to extract RNA. Subsequently, the expression levels of SNHG7 and MKL1 were determined by RT-qPCR.

#### 4.14. Hematoxylin and eosin (H&E) staining

The retina tissues of mice were fixed in 4% paraformaldehyde (Sigma) and made into paraffin sections (5-μm-thick). Paraffin slices were then dewaxed with xylene and rehydrated in a descending series of alcohol. Next, the sections were stained by hematoxylin for 5 min and eosin solution for 3 min. After dehydration with graded ethanol and permeabilization with xylene, ganglion cell layer (GCL) was observed with a microscope (Olympus, Tokyo, Japan). For analysis of GCL thickness, at least three randomly chosen fields per section were included.

#### 4.15. Statistical analysis

Graphpad Prism 7 (Graphpad, La Jolla, CA, USA) was executed to analyze all data. Data were presented as mean ± standard deviation (SD). Student's *t*-test was used to assess statistical differences between two groups. The differences among multiple groups were tested using one-way analysis of variance (ANOVA). All experiments were performed three times. *P* values <0.05 were considered statistically significant.

## 5. Conclusions

In summary, our data identified a novel role for METTL3 in regulating EndoMT in DR. We found that METTL3 and SNHG7 were downregulated in DR. Besides, METTL3 modulated m<sup>6</sup>A methylation on SNHG7 mRNA, thereafter, weakening the stability of MKL1 mRNA by binding to KHSRP. In addition, METTL3 regulated EndoMT in DR via the SNHG7/MKL1 axis. A schematic diagram of this regulatory process is outlined in Fig. 8. Our study provides novel biomarkers for DR treatment in clinic.

## Funding

This work was supported by Basic scientific research planning project of Nantong Science and Technology Bureau (project number: JC2021188).

## Ethical approval

All experiments were conducted with the approval of the Clinical Research Ethics Committee of Affiliated Hospital 2 of Nantong University, the first people's hospital of Nantong. Written informed consent was provided by the patients. All protocols of animal experiments were carried out according to the Guide for the Care and Use of Laboratory Animals of the Chinese National Institutes of Health. The current study was approved by the Animal Ethics Committee of Affiliated Hospital 2 of Nantong University, the first people's hospital of Nantong.

## Consent for publication

The informed consent was obtained from study participants.

## Availability of data and material

All data generated or analyzed during this study are included in this article. The datasets used and/or analyzed during the current study are available from the corresponding author on reasonable request.

## CRediT authorship contribution statement

**Xin Cao:** Conceptualization, Writing – original draft, Formal analysis, Funding acquisition, Writing – review & editing. **Yu Song:** Data curation, Resources. **Li-Li Huang:** Project administration, Supervision. **Ya-Jing Tian:** Investigation. **Xiao-Le Wang:** Software, Visualization. **Ling-Yan Hua:** Validation, Methodology.

## Conflict of interest

The authors declare that there is no conflict of interest.

## Data availability

No data was used for the research described in the article.

## Acknowledgements

We would like to give our sincere gratitude to the reviewers for their constructive comments.

## References

- [1] S. Vujosevic, S.J. Aldington, P. Silva, C. Hernández, P. Scanlon, T. Peto, R. Simó, Screening for diabetic retinopathy: new perspectives and challenges, *Lancet Diabetes Endocrinol.* 8 (2020) 337–347.
- [2] W. Wang, A.C.Y. Lo, Diabetic retinopathy: pathophysiology and treatments, *Int. J. Mol. Sci.* 19 (2018).
- [3] J. Lechner, O.E. O'Leary, A.W. Stitt, The pathology associated with diabetic retinopathy, *Vis. Res.* 139 (2017) 7–14.
- [4] H.P. Hammes, Diabetic retinopathy: hyperglycaemia, oxidative stress and beyond, *Diabetologia* 61 (2018) 29–38.
- [5] A. Ceriello, Point: postprandial glucose levels are a clinically important treatment target, *Diabetes Care* 33 (2010) 1905–1907.
- [6] Y. Cao, B. Feng, S. Chen, Y. Chu, S. Chakrabarti, Mechanisms of endothelial to mesenchymal transition in the retina in diabetes, *Invest. Ophthalmol. Vis. Sci.* 55 (2014) 7321–7331.
- [7] F. Lin, N. Wang, T.C. Zhang, The role of endothelial-mesenchymal transition in development and pathological process, *IUBMB Life* 64 (2012) 717–723.
- [8] Z. Li, B. Chen, W. Dong, M. Kong, Z. Fan, L. Yu, D. Wu, J. Lu, Y. Xu, MKL1 promotes endothelial-to-mesenchymal transition and liver fibrosis by activating TWIST1 transcription, *Cell Death Dis.* 10 (2019) 899.
- [9] D.F. De Jesus, Z. Zhang, S. Kahraman, N.K. Brown, M. Chen, J. Hu, M.K. Gupta, C. He, R.N. Kulkarni, M(6)a mRNA methylation regulates human  $\beta$ -cell biology in physiological states and in type 2 diabetes, *Nat. Metab.* 1 (2019) 765–774.
- [10] N. Kumari, A. Karmakar, M.M. Ahamad Khan, S.K. Ganesan, The potential role of m6A RNA methylation in diabetic retinopathy, *Exp. Eye Res.* 208 (2021), 108616.
- [11] K. Taketo, M. Konno, A. Asai, J. Koseki, M. Toratani, T. Satoh, Y. Doki, M. Mori, H. Ishii, K. Ogawa, The epitranscriptome m6A writer METTL3 promotes chemo- and radioresistance in pancreatic cancer cells, *Int. J. Oncol.* 52 (2018) 621–629.
- [12] Y. Yang, F. Shen, W. Huang, S. Qin, J.T. Huang, C. Sergi, B.F. Yuan, S.M. Liu, Glucose is involved in the dynamic regulation of m6A in patients with type 2 diabetes, *J. Clin. Endocrinol. Metab.* 104 (2019) 665–673.
- [13] J. Yang, J. Liu, S. Zhao, F. Tian, N(6)-Methyladenosine METTL3 modulates the proliferation and apoptosis of lens epithelial cells in diabetic cataract, *Mol. Ther. Nucl. Acids* 20 (2020) 111–116.
- [14] X. Zha, X. Xi, X. Fan, M. Ma, Y. Zhang, Y. Yang, Overexpression of METTL3 attenuates high-glucose induced RPE cell pyroptosis by regulating miR-25-3p/PTEN/Akt signaling cascade through DGCR8, *Aging* 12 (2020) 8137–8150.
- [15] H. Yu, Z. Zhang, ALKBH5-mediated m6A demethylation of lncRNA RMRP plays an oncogenic role in lung adenocarcinoma, *Mamm. Genome* 32 (2021) 195–203.
- [16] Y. Fang, M.J. Fullwood, Roles, functions, and mechanisms of long non-coding RNAs in cancer, *Genom. Proteome. Bioinform.* 14 (2016) 42–54.
- [17] Y. He, Y. Dan, X. Gao, L. Huang, H. Lv, J. Chen, DNMT1-mediated lncRNA MEG3 methylation accelerates endothelial-mesenchymal transition in diabetic retinopathy through the PI3K/Akt/mTOR signaling pathway, *Am. J. Physiol. Endocrinol. Metab.* 320 (2021) E598–e608.
- [18] A.A. Thomas, S. Biswas, B. Feng, S. Chen, J. Gonder, S. Chakrabarti, lncRNA H19 prevents endothelial-mesenchymal transition in diabetic retinopathy, *Diabetologia* 62 (2019) 517–530.
- [19] M.A. Chaudhry, Expression pattern of small nucleolar RNA host genes and long non-coding RNA in X-rays-treated lymphoblastoid cells, *Int. J. Mol. Sci.* 14 (2013) 9099–9110.
- [20] X. Cao, L.D. Xue, Y. Di, T. Li, Y.J. Tian, Y. Song, MSC-derived exosomal lncRNA SNHG7 suppresses endothelial-mesenchymal transition and tube formation in diabetic retinopathy via miR-34a-5p/XBP1 axis, *Life Sci.* 272 (2021), 119232.
- [21] M. Corley, M.C. Burns, G.W. Yeo, How RNA-binding proteins interact with RNA: molecules and mechanisms, *Mol. Cell* 78 (2020) 9–29.
- [22] M.L. Zuo, A.P. Wang, Y. Tian, L. Mao, G.L. Song, Z.B. Yang, Oxymatrine ameliorates insulin resistance in rats with type 2 diabetes by regulating the expression of KSRP, PETN, and AKT in the liver, *J. Cell. Biochem.* 120 (2019) 16185–16194.
- [23] L. Mao, L. Liu, T. Zhang, X. Wu, T. Zhang, Y. Xu, MKL1 mediates TGF- $\beta$ -induced CTGF transcription to promote renal fibrosis, *J. Cell. Physiol.* 235 (2020) 4790–4803.
- [24] Y. Ding, H. Xu, L. Li, Y. Yuan, Y. Xu, Megakaryocytic leukemia 1 (MKL1) mediates high glucose induced epithelial-mesenchymal transition by activating LOX transcription, *Biochem. Biophys. Res. Commun.* 509 (2019) 633–640.
- [25] V.M. Villegas, S.G. Schwartz, Current and future pharmacologic therapies for diabetic retinopathy, *Curr. Pharm. Des.* 24 (2018) 4903–4910.
- [26] F. Semeraro, A. Cancarini, R. dell'Omo, S. Rezzola, M.R. Romano, C. Costagliola, Diabetic retinopathy: vascular and inflammatory disease, *J. Diabetes Res.* 2015 (2015), 582060.
- [27] F. Gui, Z. You, S. Fu, H. Wu, Y. Zhang, Endothelial dysfunction in diabetic retinopathy, *Front. Endocrinol.* 11 (2020) 591.
- [28] T. Sun, R. Wu, L. Ming, The role of m6A RNA methylation in cancer, *Biomed. Pharmacother.* 112 (2019), 108613.
- [29] Y. Yuan, Y. Du, L. Wang, X. Liu, The M6A methyltransferase METTL3 promotes the development and progression of prostate carcinoma via mediating MYC methylation, *J. Cancer* 11 (2020) 3588–3595.
- [30] H. Hu, Q. Kong, X.X. Huang, H.R. Zhang, K.F. Hu, Y. Jing, Y.F. Jiang, Y. Peng, L. C. Wu, Q.S. Fu, L. Xu, Y.B. Xia, Longnon-coding RNA BLACAT2 promotes gastric cancer progression via the miR-193b-5p/METTL3 pathway, *J. Cancer* 12 (2021) 3209–3221.
- [31] L. Xue, J. Li, Y. Lin, D. Liu, Q. Yang, J. Jian, J. Peng, m(6) A transferase METTL3-induced lncRNA ABHD11-AS1 promotes the Warburg effect of non-small-cell lung cancer, *J. Cell. Physiol.* 236 (2021) 2649–2658.
- [32] M.D. Yao, Q. Jiang, Y. Ma, C. Liu, C.Y. Zhu, Y.N. Sun, K. Shan, H.M. Ge, Q. Y. Zhang, H.Y. Zhang, J. Yao, X.M. Li, B. Yan, Role of METTL3-dependent N(6)-methyladenosine mRNA modification in the promotion of angiogenesis, *Mol. Ther.* 28 (2020) 2191–2202.
- [33] W. Jiang, P. Zhu, F. Huang, Z. Zhao, T. Zhang, X. An, F. Liao, L. Guo, Y. Liu, N. Zhou, X. Huang, The RNA methyltransferase METTL3 promotes endothelial progenitor cell angiogenesis in mandibular distraction osteogenesis via the PI3K/AKT pathway, *Front. Cell Dev. Biol.* 9 (2021), 720925.
- [34] X. Tan, W.B. Chen, D.J. Lv, T.W. Yang, K.H. Wu, L.B. Zou, J. Luo, X.M. Zhou, G. C. Liu, F.P. Shu, X.M. Mao, lncRNA SNHG1 and RNA binding protein hnRNPL form a complex and coregulate CDH1 to boost the growth and metastasis of prostate cancer, *Cell Death Dis.* 12 (2021) 138.
- [35] P. Briata, D. Bordo, M. Puppo, F. Gorlero, M. Rossi, N. Perrone-Bizzozero, R. Gherzi, Diverse roles of the nucleic acid-binding protein KHSRP in cell differentiation and disease, *Wiley interdisciplinary reviews, RNA* 7 (2016) 227–240.
- [36] Q. Gou, L. Gao, X. Nie, W. Pu, J. Zhu, Y. Wang, X. Liu, S. Tan, J.K. Zhou, Y. Gong, J. He, K. Wu, Y. Xie, W. Zhao, L. Dai, L. Liu, R. Xiang, Y.Q. Wei, L. Zhang, Y. Peng, Long noncoding RNA AB074169 inhibits cell proliferation via modulation of KHSRP-mediated CDKN1a expression in papillary thyroid carcinoma, *Cancer Res.* 78 (2018) 4163–4174.
- [37] M.E. McDonald, C. Li, H. Bian, B.D. Smith, M.D. Layne, S.R. Farmer, Myocardin-related transcription factor a regulates conversion of progenitors to beige adipocytes, *Cell* 160 (2015) 105–118.
- [38] H. Xu, X. Wu, H. Qin, W. Tian, J. Chen, L. Sun, M. Fang, Y. Xu, Myocardin-related transcription factor a epigenetically regulates renal fibrosis in diabetic nephropathy, *J. Am. Soc. Nephrol.* 26 (2015) 1648–1660.
- [39] K. Hu, J.L. Li, X.W. Yuan, MicroRNA-411 plays a protective role in diabetic retinopathy through targeted regulating Robo4, *Eur. Rev. Med. Pharmacol. Sci.* 23 (2019) 9171–9179.
- [40] S. Biswas, A.A. Thomas, S. Chen, E. Aref-Eshghi, B. Feng, J. Gonder, B. Sadikovic, S. Chakrabarti, MALAT1: an epigenetic regulator of inflammation in diabetic retinopathy, *Sci. Rep.* 8 (2018) 6526.